Atomic Force and Scanning Electron Microscopy of Atmospheric Particles

ZAHAVA BARKAY,[1]* AMIT TELLER,[2] ELIEZER GANOR,[2] ZEV LEVIN,[2] AND YORAM SHAPIRA[3]
[1]*Wolfson Applied Materials Research Center, Tel-Aviv University, Ramat Aviv 69978, Israel*
[2]*Department of Geophysics and Planetary Sciences, Raymond and Beverly Sackler Faculty of Exact Sciences, Tel-Aviv University, Ramat Aviv 69978, Israel*
[3]*Department of Electrical Engineering, The Iby and Aladar Fleischman Faculty of Engineering, Tel-Aviv University, Ramat Aviv 69978, Israel*

KEY WORDS atmospheric aerosols; atomic force microscopy; scanning electron microscopy; energy dispersive spectroscopy

ABSTRACT Atomic force microscopy (AFM) and scanning electron microscopy with energy dispersive spectroscopy (SEM–EDS) have been used for both morphological and elemental mass analysis study of atmospheric particles. As part of the geometrical particle analysis, and in addition to the traditional height profile measurement of individual particles, AFM was used to measure the volume relative to the projection area for each particle separately, providing a particle shape model. The element identification was done by the EDS analysis, and the element mass content was calculated based on laboratory calibration with particles of known composition. The SEM–EDS mass measurements from two samples collected at 150 and 500 m above the surface of the Mediterranean Sea were found to be similar to mass calculations derived from the AFM volume measurements. The AFM results show that the volume of most of the aerosols that were identified as soluble marine sulfate and nitrate aerosol particles can be better estimated using cylindrical shapes than spherical or conical geometry. *Microsc. Res. Tech. 68:107–114, 2005.*

INTRODUCTION

Analysis of individual particles using scanning electron microscopy (SEM) is frequently conducted so as to characterize atmospheric aerosols from anthropogenic (pollution) and natural (sea salt, mineral dust, etc.) sources (Spurny, 1986).

A calibration technique for calculating the mass of different chemical elements in individual particles using energy dispersive spectroscopy (EDS) in SEM was developed (Pardess et al., 1992; Levin et al., 1996). The method was used to identify the composition of particles of different sources, in ambient air and in clouds (Falkovich et al., 2001; Levin et al., 1990). The information obtained using SEM–EDS serves to correlate between the chemical and morphological properties of atmospheric particles.

One important deficiency of the SEM characterization is the inability to explore the three-dimensional (3D) morphology of the particles and thus assume that the investigated particles on the substrates are hemispherical. The morphology of atmospheric particles received significant importance in recent years due to the effect of the particles' shape on their radiative properties. Wang et al. (2003) and Kalashnikova and Sokolik (2002), for example, studied the role of the nonspherical shape of dust particles on their optical properties. The role of the particles' shape is sufficiently large as to affect the retrievals of aerosol optical properties from satellite and ground-based remote sensing observations.

It is clear that there is a need to incorporate new and better analytical tools in the investigation of aerosols, such that the particle geometry is obtained in 3D simultaneously with compositional information. In recent years, AFM became a valuable complementary method to the SEM, for the study of the geometrical features of particles in various fields of material research, including environmental science (Posfai et al., 1998; Ramirez-Aguilar et al., 1999).

In this study, the AFM is presented as a complementary method to SEM for both morphological and particle mass estimation. AFM has several advantages over SEM concerning the morphological diagnostics of atmospheric aerosol samples. The use of the AFM in the noncontact mode permits analysis of aerosol particles without charging and heating problems, resulting in reduced morphological changes during the analysis. By using AFM, the sample is investigated at room environmental conditions, without vacuum. Finally, the 3D AFM structural information complements the two-dimensional (2D) information of the SEM for a full-shape characterization, with 0.1 nm height and a few nanometers lateral resolutions. By using these advantages, several AFM morphological measurements were reported in recent years for environmental

*Correspondence to: Dr. Zahava Barkay, Wolfson Applied Materials Research Center, Tel-Aviv University, Ramat Aviv 69978, Israel.
E-mail: barkay@post.tau.ac.il

Received 18 May 2005; accepted in revised form 31 August 2005

Contract grant sponsor: Porter School of Environmental Studies at Tel-Aviv University, Israel.

DOI 10.1002/jemt.20241

Published online in Wiley InterScience (www.interscience.wiley.com).

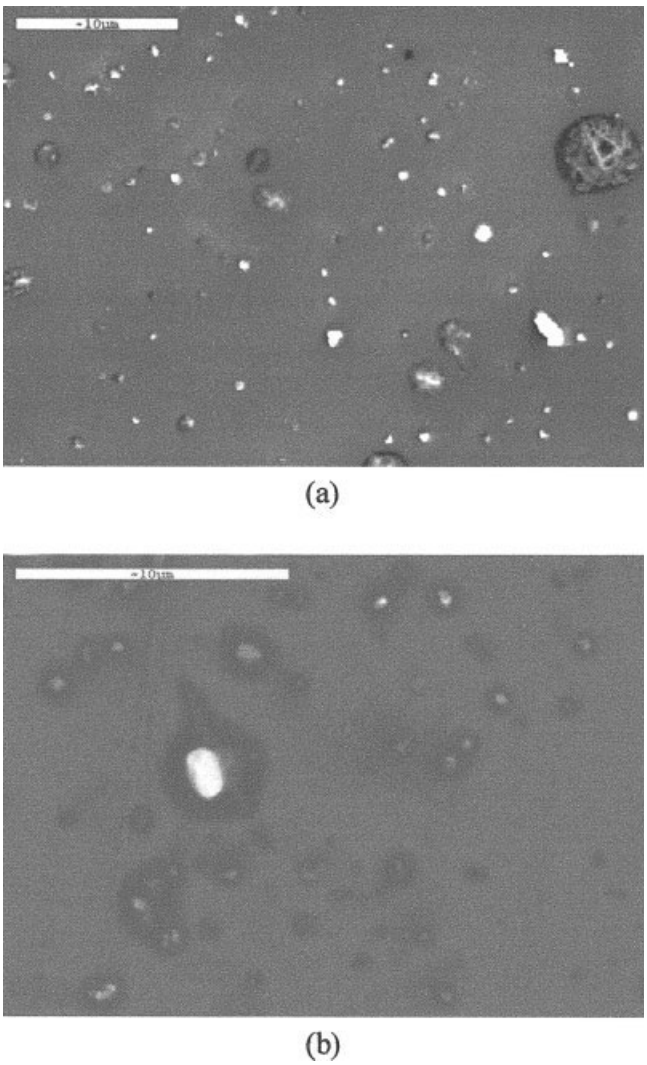

Fig. 1. SEM images of particles: (**a**) 150 m altitude and (**b**) 500 m altitude.

particles (Kollensperger et al., 1999; Posfai et al., 1998; Ramirez-Aguilar et al., 1999; Vaz et al., 2002).

In this work, the particle volume has been measured directly from the 3D AFM values, and the particle shape has been modeled by the ratio of the particle volume to the projection area. Furthermore, we apply the particles' volume measurements to their mass calculations. Finally, the particle mass obtained by AFM is correlated with SEM–EDS mass calculations of the same samples.

MATERIALS AND METHODS

Particle Sampling and Preparation

For the present study, and as an example of the use of the method, we analyzed aerosol samples that were collected using a single-stage impactor, mounted on a King-Air airplane, which performed research flights in Crete in the summer of 2001, as part of the Mediterranean Intensive Oxidant Study (MINOS). This campaign was aimed to characterize the size and composition of atmospheric aerosols transported from distant sources and to investigate their effects on the climate of the Mediterranean region. (Lelieveld et al., 2002).

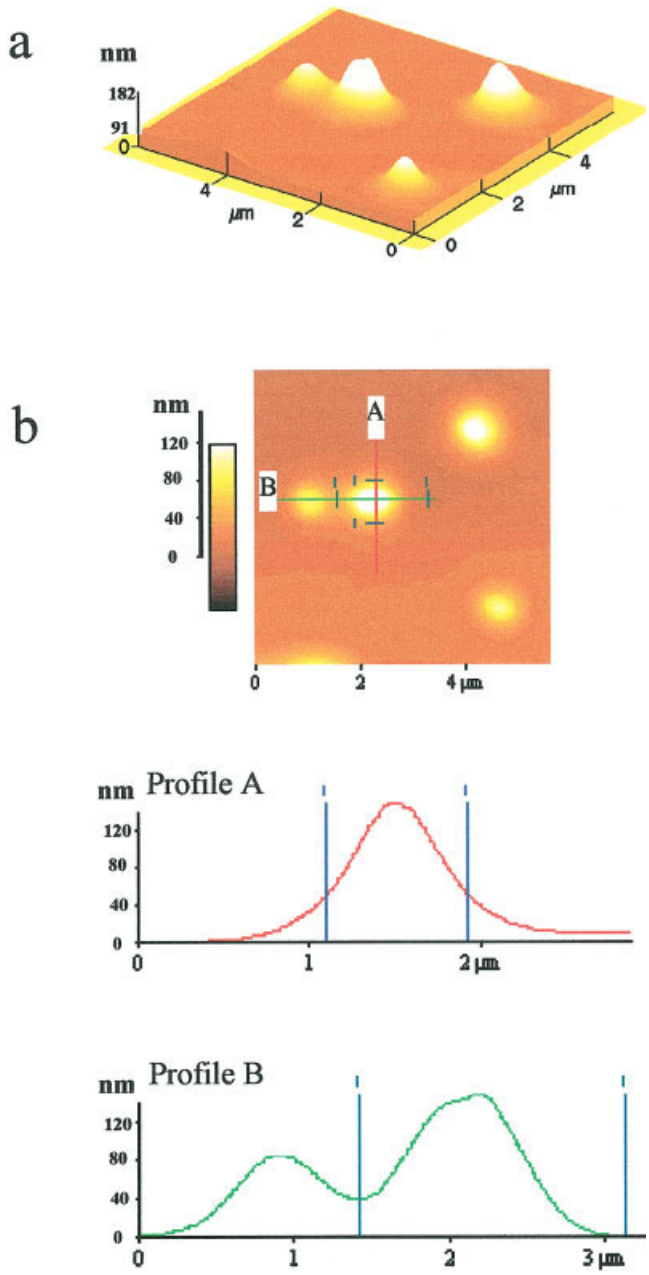

Fig. 2. AFM images of particles at 150 m altitude: (**a**) 3D image and (**b**) 2D image and line profiles.

The single-stage impactor was placed in the airplane as part of a specially designed sampling system. The size and the diameters of the sampling inlet and the tubes were designed according to the flow rate requirements of the impactor and the demand for isokinetic flow based on the calculations presented previously by others (Kouimtzis and Samara, 1995). Comprehensive description of the sampling system and its components is discussed by Levin et al. (2005).

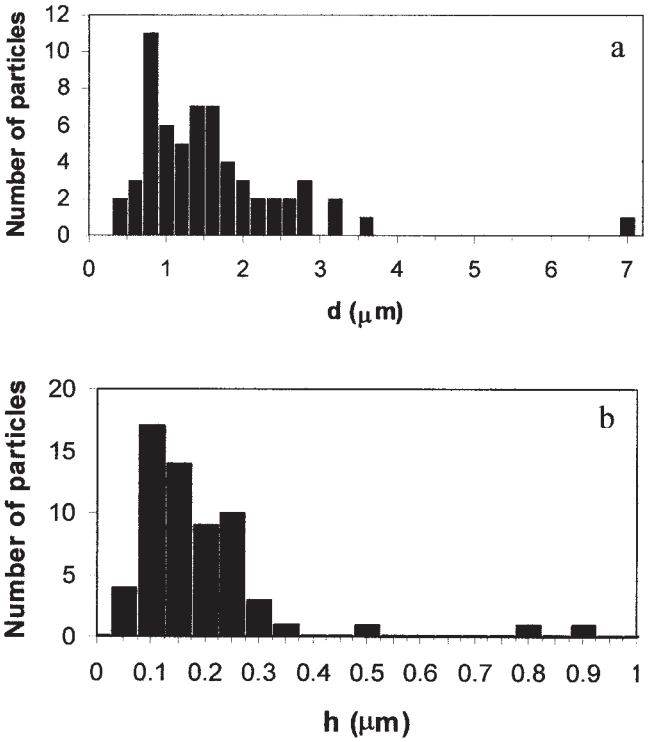

Fig. 3. The particle diameter (**a**) and height (**b**) histograms for 150 m altitude.

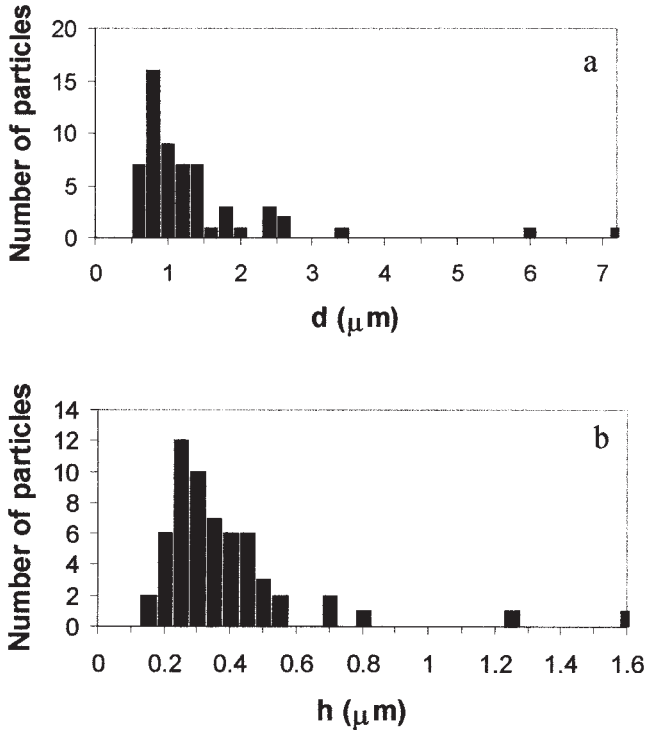

Fig. 4. The particle diameter (**a**) and height (**b**) histograms for 500 m altitude.

The single-stage impactor was used to collect particles on electron microscope grids. Typical sampling time was ~2 min for a grid. The grids were precoated with a thick layer of carbon so as to differentiate droplets from dry aerosols by identifying the ringed dark imprint around the droplets (Ganor and Pueschel, 1988), and by studying the particles individually, to identify their shape and elemental composition.

TABLE 1. Possible particle shape models according to V/A

Shape	Volume V	Projection area A	V/A
Cylinder (vertical axis perpendicular)	$\pi r^2 h$	πr^2	h
Cylinder (vertical axis parallel)	$\pi r h^2/2$	$2hr$	$\pi h/4$
Cone	$\pi r^2 h/3$	πr^2	$h/3$
Half sphere	$2\pi r^3/3$	πr^2	$2r/3$

Methods and Analysis

The analysis consisted of finding the elemental mass of different particles by using a calibration method (Levin et al., 1996; Pardess et al., 1992). With this method, one could estimate the elemental mass by comparing the X-ray counts of the inspected particles with the counts of calibrated particles of known masses. For particles < 0.4 μm, the X-ray counts from the different elements in the EDS analysis are similar to the background noise, and therefore, our EDS analysis is applicable only for particles > 0.4 μm. The analysis identified the following elements: Na, Mg, Al, Si, S, K, Cl, Ca, and Fe. The samples were collected on Thermanox substrate. Since Thermanox contains carbon, the present method could not identify this element in the particle. The mass of nitrogen was estimated only qualitatively being a low atomic element of close proximity to the carbon in the X-ray spectrum.

The present study concentrates on samples that were collected in the atmospheric boundary layer at altitudes of 150 and 500 m above the sea level (ASL). These altitudes are characterized by internal and external mixture of aerosols from marine and air-pollution sources. In addition, our samples revealed the presence of a few pure mineral dust particles at these altitudes.

The atomic force microscope is a Park Scientific Instruments model M5 with a Proscan image-processing software. The samples were examined using noncontact AFM mode with UL20B cantilevers and conical tips of 10 nm radius and 12° angle. The SEM is a JSM-6300 with an Oxford EDS system. The EDS system uses Si detector of 138 eV resolution at 5.9 KeV and ultra-thin window. The elemental analysis software is ISIS-Link Oxford.

On entering the impactor, the particles are collected on the grid's surface with the largest ones just under the middle of the airflow, while smaller particles are deflected sideways and impact the substrate a small distance away from center. This produces a visible strip of deposited particles that is recognized by eye or in low magnification optical microscope, which is mounted on the AFM and allows easy identification of the desired sample regions. By using SEM, the particle diameter is measured directly on the secondary electron (SE) image. By using AFM, a general image of the particles is taken at ~20-μm full scan size, which

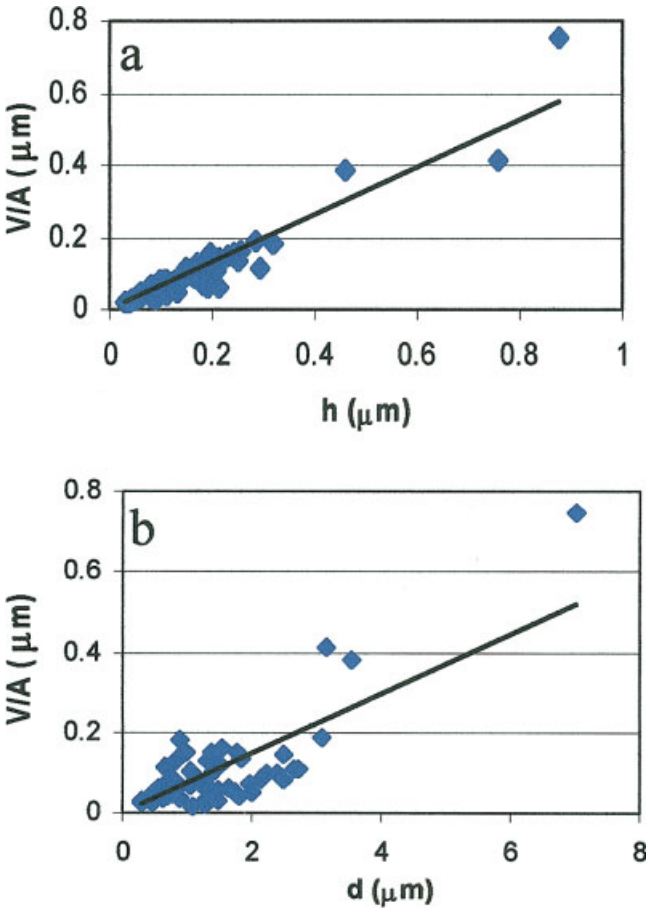

Fig. 5. Particle shape at 150 m altitude using AFM: (**a**) volume to projection area dependence on particle height and (**b**) volume to projection area dependence on particle diameter. [Color figure can be viewed in the online issue, which is available at www.interscience.wiley.com.]

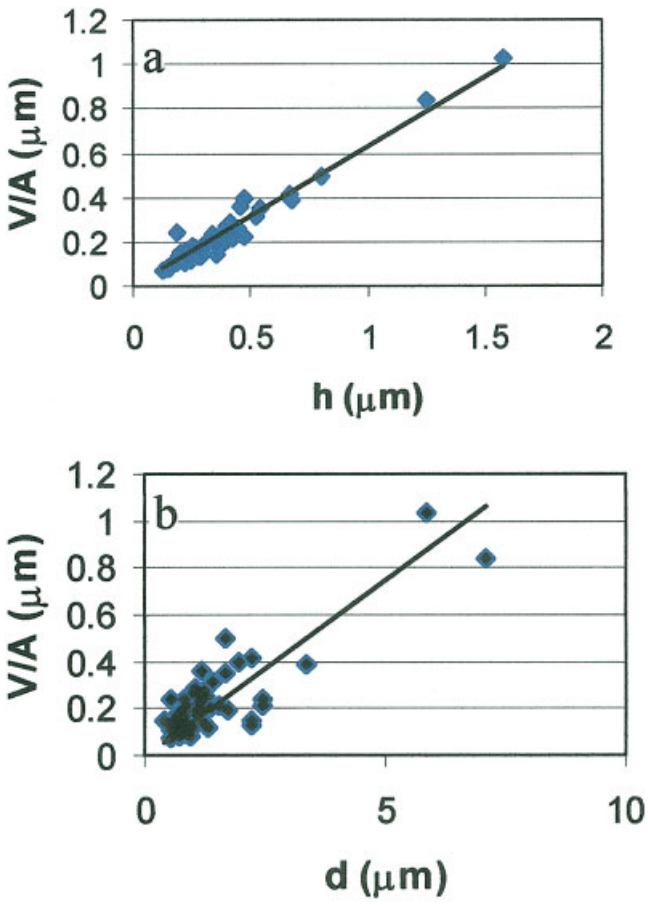

Fig. 6. Particle shape at 500 m altitude using AFM: (**a**) volume to projection area dependence on particle height and (**b**) volume to projection area dependence on particle diameter. [Color figure can be viewed in the online issue, which is available at www.interscience.wiley.com.]

generally includes 5–10 particles depending on the exact location. Then, the individual particles are magnified so as to measure the height and diameter, as well as the volume and projection area (after background subtraction). The shape of the particular AFM tips that are used provides a high lateral resolution and precise particle slope angles up to 78°, which is much higher than the measured values. In our study, superimposed particles are excluded from the analysis. The SEM and AFM analysis of individual particles is carried out on ~100 particles for each sample.

RESULTS

Particle Volume and Shape Estimation

SEM images of atmospheric aerosols from the two samples are shown in Figures 1a and 1b. The Figures show that the diameters of most of the sampled particles are between 0.5 and 3 μm. The 2D geometrical information from the SEM images cannot reveal the full particle shape and volume, and therefore, it is extended to 3D information by the AFM analysis. Because of the impaction of the particle and their smearing on the substrate, the aerosols are modified toward a more elliptical shape. This effect is seen in some of particles in Figures 1a and 1b. Figure 2a also demonstrates this effect showing a 3D AFM image of submicron to micron size particles collected at 150 m above the sea. Figure 2b represents the corresponding 2D image with height profiles. The points, which are marked as "1" at profile A at both sides of the particle, correspond to ~50 nm height relative to background and are positioned at a place in which the slope changes by a factor of 2.5 (from 19° to 7°) across the particle from center to edge. The exact values of the slope change at the particle surface from center to edge are particle dependent. This phenomenon is also shown in profile B. In addition, the nonzero height between the particles is interpreted as particle smearing on the substrate. This undefined edge of the particle is a source of uncertainty in the particle diameter estimation using the SE contrast in SEM. This is in addition to the change in SE contrast within the particle. The

TABLE 2. Particle shape fit to AFM results for 150 and 500 m samples

Sample (m)	Diameter fit curve (V/A)	Diameter fit coefficient (R^2)	Height fit curve (V/A)	Height fit coefficient (R^2)
150	$0.07d$	0.626	$0.66h$	0.894
500	$0.15d$	0.659	$0.63h$	0.955

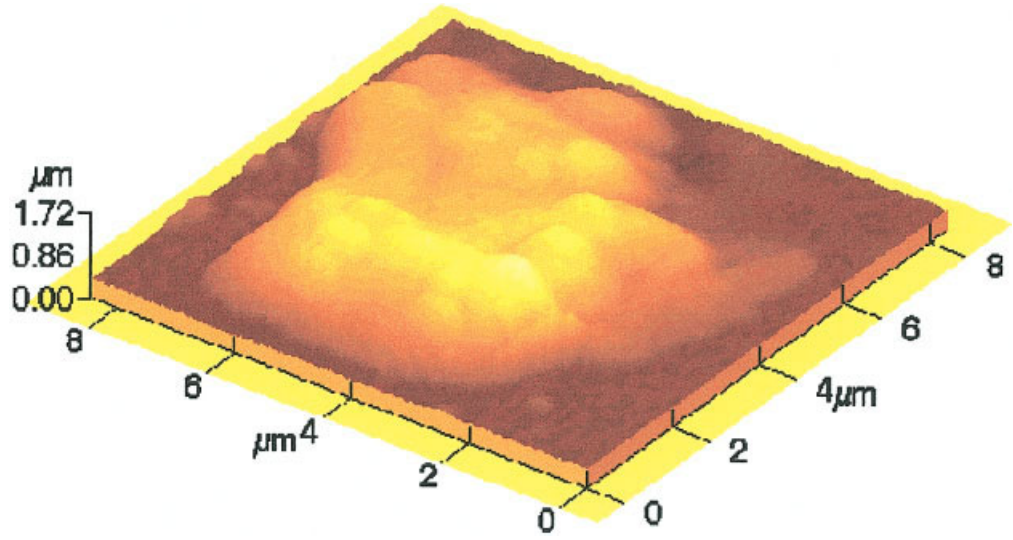

Fig. 7. 3D AFM image of a large particle at 500 m altitude.

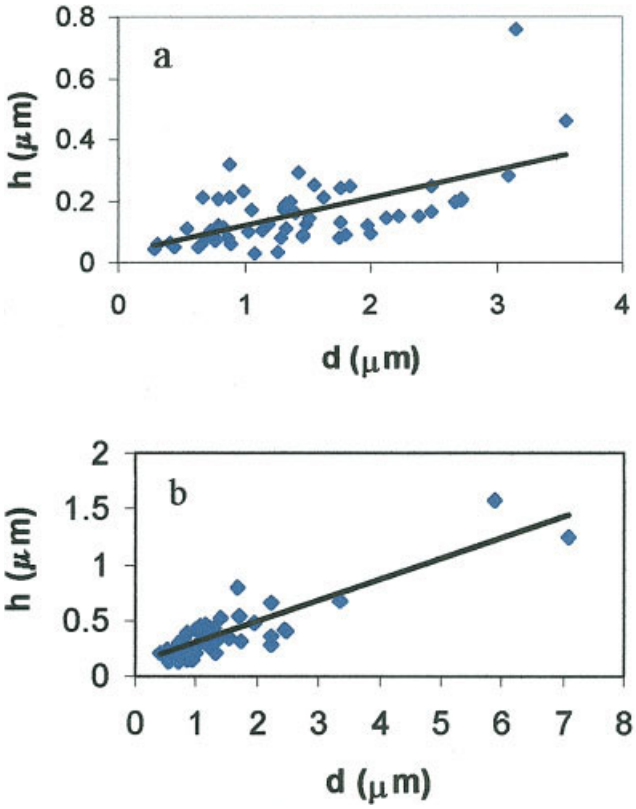

Fig. 8. Height versus diameter for particles shown in Figures 3 and 4: (**a**) 150 m altitude and (**b**) 500 m altitude.

histograms of the average particle diameter and maximum height are shown in Figures 3 and 4 for 150 and 500 m altitudes, respectively. Figure 3 shows that the most probable value for particles at altitude of 150 m is 0.8 μm in diameter (Fig. 3a) and 0.1 μm in height (Fig. 3b), while Figure 4 shows that the most probable value for particles at altitude of 500 m is 0.8 μm in diameter (Fig. 4a) and 0.25 μm in height (Fig. 4b). Figure 3a shows relatively high fraction of particles larger than 2 μm (~25% of the entire analyzed particles). In Figure 4a, the fraction of these particles (defined here as coarse mode aerosols) is smaller. These results indicate some differences in size and possibly in shape between the aerosol properties at the two heights. The higher concentration of coarse particles at 150 m, as compared with that at 500 m, is a result of their sedimentation from the higher to the lower levels.

The particles shown in Figure 2a appear to have conical shapes. However, the particle height scale is an order of magnitude lower than the lateral scale; therefore, in reality, the particles could be regarded as hemispheric or cylinders lying on their side. The particle shape model is obtained by measuring the exact volume (V), based on the 3D AFM data, relative to the projection area (A) of each particle separately. Table 1 shows the V/A dependence on the maximal height and radius for four possible particle shape models such as cylinder (with vertical axis perpendicular and parallel to the surface), cone, and hemisphere.

Figures 5 and 6 show the results for the samples taken at 150 and 500 m altitudes, respectively. Figures 5a and 6a show V/A as a function of maximal particle height, and Figures 5b and 6b show V/A as a function of diameter with suitable linear fitting curves. Table 2 shows the fitting equations for the measured V/A values as a function of diameter and height with the corresponding fit coefficients. The Table shows that relatively higher fit coefficients to the data are obtained for the dependence of V/A on height than of V/A to diameter. Comparison to Table 1 reveals that the fitted slope values of about 2/3 (in Table 2) correspond to aerosol particle of cylindrical-type with vertical axis parallel to the surface in which the V/A ratio versus h is $\pi/4$ (~0.78). Therefore, the shape of the particles fits better to a cylindrical shape than to other shapes. Figure 7 shows a coarse mode particle from the sample taken at 150 m. The Figure indicates that a fraction of the

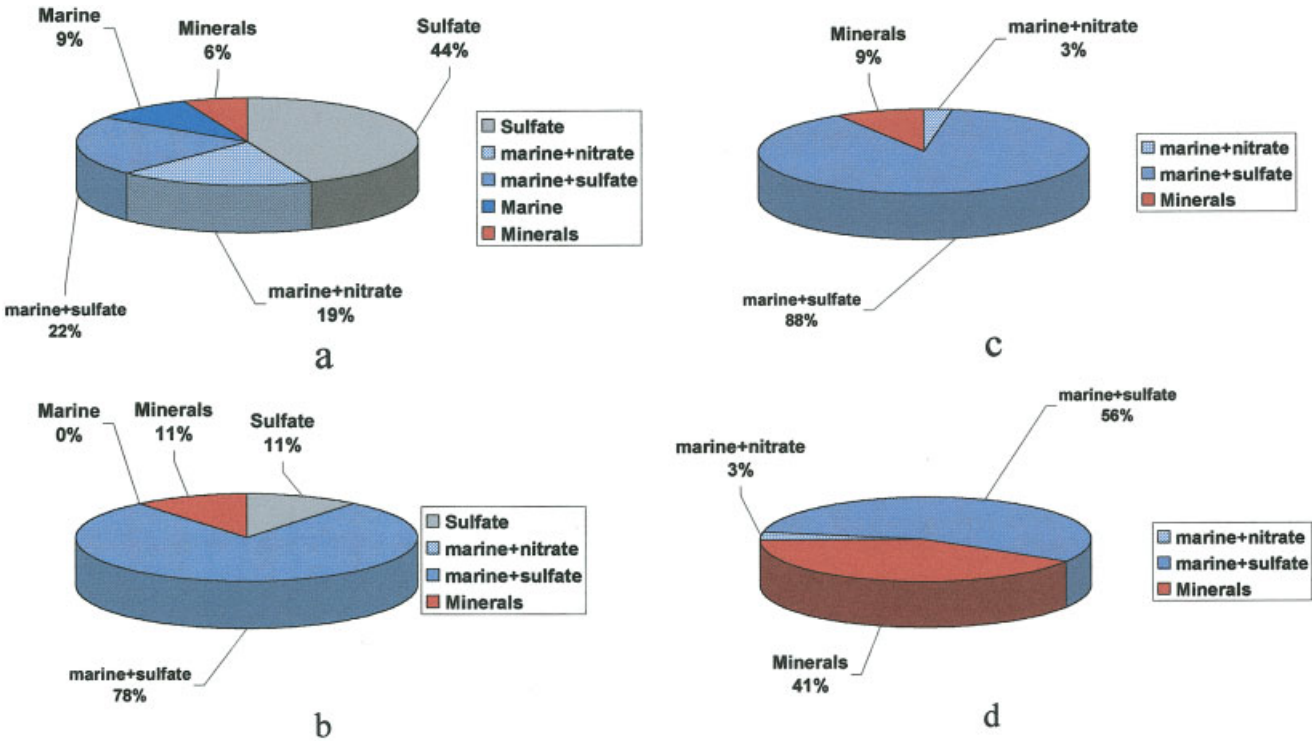

Fig. 9. Frequency distribution of different aerosol types for fine (<1 μm) and coarse (>1 μm) particles: (**a**) fine particles at altitude 150 m, (**b**) coarse particles at altitude 150 m, (**c**) fine particles at altitude 500 m, and (**d**) coarse particles at altitude 500 m. [Color figure can be viewed in the online issue, which is available at www.interscience.wiley.com.]

coarse particles (a few microns in diameter) are actually aggregates of several particles.

The difference in fit coefficients for *V/A* versus height in comparison to *V/A* versus diameter shows that the height and diameter are not highly correlated in the range of submicron- to micron-size particles. This is shown explicitly in the height versus diameter graphs of Figure 8a with fitted slope of 0.1 and fitted index of 0.36, and 8(b) with fitted slope of 0.18 and fitted index of 0.77. The lower fitted index in Figure 8a relative to Figure 8b is due to the contribution of a few coarse aggregated particles.

Particles Mass Estimation

The elemental composition of the individual particles was analyzed using SEM–EDS as described previously (Levin et al., 1996; Pardess et al., 1992).

The analyzed particles were divided into five groups based on their heavy-element chemical composition and their elemental masses. The groups were as follows:

1. Marine aerosols—These particles contained sodium and chloride and were associated with sea salt (NaCl). Magnesium was also identified in many of the marine particles.
2. Sulfate—Particles containing only sulfur were identified as sulfate aerosols. These particles could be associated with sulfuric acid (H_2SO_4), ammonium sulfate $(NH_4)SO_4$, or NH_3HSO_4.
3. Marine-sulfate—Particles containing sodium and sulfate were associated with reaction products of sulfate aerosols such as sulfuric acid with sodium-chloride to form sodium-sulfate (Na_2SO_4). Some particles containing Na, small mass of Cl, and large mass of S were also classified in this category.
4. Marine-nitrate—Particles containing only Na with no Cl or very small mass of chlorine were associated with reaction products of nitrate with marine aerosols to form sodium-nitrate ($NaNO_3$). It is assumed that these particles are products of chemical reaction of NaCl with NO_3 as discussed by Levin et al. (2005).
5. Minerals—Particles containing Al, Si, Ca, and Fe were identified as minerals.

Figure 9a–9d presents aerosol classification of 130 particles from the two samples according to the above groups separated to fine mode (<1 μm) and coarse mode (>1 μm). Figures 9a and 9b show the classification for the sample that was collected at 150-m ASL for the fine and the coarse mode, respectively. Figures 9c and 9d show the classification for the sample that was collected at 500-m ASL.

Most of the particles in both the fine and the coarse mode were identified by the EDS as marine aerosols or mixture of marine aerosols with air pollution (sulfate or nitrate). The analysis reveals that in the sample collected at 500–m, as compared with that collected at 150–m, the fraction of minerals dust particles is larger and especially in the coarse mode (Fig. 9d). In addition, more pure sulfate aerosols were found at the lower altitude. These particles are assumed to be composed of

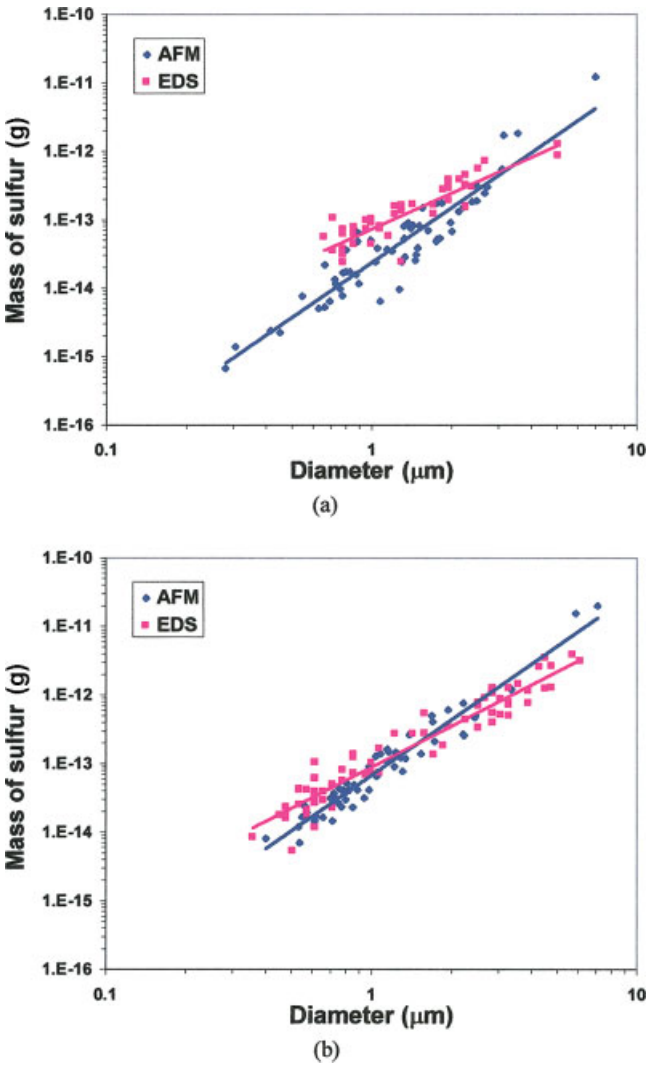

Fig. 10. Sulfur mass of particles: (**a**) at 150 m altitude and (**b**) 500 m altitude. [Color figure can be viewed in the online issue, which is available at www.interscience.wiley.com.]

TABLE 3. Sulfur mass fit-curves for AFM and EDS measurements at 150 and 500 m altitudes

Sample (m)	EDS fit curve (M)	EDS fit coefficient (R^2)	AFM fit curve (M)	AFM fit coefficient (R^2)
150	$7 \times 10^{-14} d^{1.74}$	0.805	$2 \times 10^{-14} d^{2.66}$	0.874
500	$9 \times 10^{-14} d^{1.99}$	0.924	$7 \times 10^{-14} d^{2.68}$	0.942

sulfuric-acid, which did not react with sea salt due to the short-time that passed from the release of the sea salt particles from the sea surface. Since most particles in our measurements both in 150 and 500 m contained Na and S, we assume for the present mass calculations that the particles were all composed of Na_2SO_4. The above assumption is made because such particles are very common in the atmosphere and it is in line with the present results showing that the fraction of Na and S in the samples is large (Fig. 9). The density of Na_2SO_4 is 2.68 g cm^{-3}. Since the mass of S makes up 23% of the Na_2SO_4 mass, one can calculate the amount of S from the volume estimation from AFM and compare with the mass of S as measured directly by the SEM–EDS.

Figures 10a and 10b show the sulfur mass as a function of the particle diameter for both AFM and SEM–EDS measurements for the 150 and 500 m samples, respectively. The measured values are presented together with the fitted curves in both Figures. Table 3 shows that the AFM slope values are higher than the SEM–EDS for both altitudes. Thus, at the altitude of 150 m, the amount of sulfur based on SEM–EDS is higher for all particles below 4-μm diameter. The measured sulfur at 500 m gives higher SEM–EDS values for particles below 1–2 μm in diameter.

DISCUSSION

Our AFM analysis uses the particles volumes for calculating the sulfur mass; here, we assumed that the sampled particles were composed of only Na_2SO_4. However, particles with no sulfur could be included in the calculation. This last assumption contributes to the deviations between the SEM–EDS and the AFM measurements. The differences between Figures 10a and 10b show the drawback of the assumption that all aerosols are composed of sodium-sulfate. In the sample that was taken at 150 m (Fig. 10a), many of the fine mode particles were sulfate; therefore, the sulfur mass fraction should be >23% at the smaller diameters, and the line of the AFM analysis should have smaller slope. The slope of the AFM analysis of sulfur mass in Figure 10b should also be smaller, because in the sample that was taken at 500 m, many of the coarse mode particles were composed of minerals (41%) and the fraction of sulfur should have decreased. It has been also shown before (Levin et al., 1996) that, when mineral dust interacts with pollution, many of the particles get coated with sulfate. Thus, taking into account the more detailed chemical composition of the aerosols in the sulfur mass calculation should decrease the differences between the SEM and AFM measurements.

Although the SEM–EDS accurately measures the elemental composition, it fails to provide a good estimate of the volume. In contrast, the AFM provides a good estimate of the volume, but it needs to rely on a reasonable knowledge of the composition of the particles so as to assume or derive particles' density. According to the AFM dimension resolution, the precision of the mass measurement of a sulfur particle is estimated to be $\sim 10^{-21}$ g, which is several orders of magnitude lower than the typical particle masses in the samples. From this aspect, the AFM method thus provides a high accuracy for nanometer-sized particles, while the SEM–EDS measurements are more accurate for larger particles.

The aim of the present study is to explore the potential of AFM to provide a better estimation of particle shape and mass of atmospheric aerosols collected on substrates. Because of the impaction method of the particle collection over the grid surface, the spherical shape of the aerosols in the atmosphere is modified keeping the volume somewhat unaffected. Our model shows that the cylindrical shapes provide a better fit to the particles' volume than other shapes. The shape model presented here is based on AFM

geometrical data and complements the information obtained from the SEM. It is also shown that the height and diameter of the measured air pollution particles have a low linear correlation over the submicron to micron particle diameter range. Thus, any quantitative analysis must take into account the particle height in addition to the particle diameter.

CONCLUDING COMMENTS

We compared the AFM and SEM–EDS techniques for evaluating the dependence of the sulfur mass in the particles on their diameter. The results show that in spite of the differences in methods for determining the mass calculation, the sulfur mass content from the SEM–EDS and the AFM measurements are within one order of magnitude from each other. Our results thus show that AFM can serve as a complementary method to SEM for determining both morphology and mass of the particles.

REFERENCES

Falkovich AH, Ganor E, Levin Z, Formenti P, Rudich Y. 2001. Chemical and mineralogical analysis of individual mineral dust particles. J Geophys Res 106:18029–18036.

Ganor E, Pueschel RF. 1988. Composition of individual nitrate containing particles in non-urban atmospheres of Colorado, USA and Tel Aviv, Israel. Water Air Soil Pollut 42:169–181.

Kalashnikova OV, Sokolik IN. 2002. Importance of shapes and compositions of wind-blown dust particles for remote sensing at solar wavelengths. Geophys Res Lett 29:doi:10.1029/2002GL014947.

Kollensperger G, Friedbacher G, Krammer A, Grasserbauer M. 1999. Application of atomic force microscopy to particle sizing. Fresenius J Anal Chem 363:323–332.

Kouimtzis T, Samara C. 1995. Airborne particulate matter. Berlin: Springer.

Lelieveld J, Berresheim H, Borrmann S, Crutzen PJ, Dentener FJ, Fischer H, Feichter J, Flatau PJ, Heland J, Holzinger R, Korrmann R, Lawrence MG, Levin Z, Markowicz KM, Mihalopoulos N, Minikin A, Ramanathan V, de Reus M, Roelofs GJ, Scheeren HA, Sciare J, Schlager H, Schultz M, Siegmund P, Steil B, Stephanou EG, Stier P, Traub M, Warneke C, Williams J, Ziereis H. 2002. Global air pollution crossroads over the Mediterranean. Science 298:794–799.

Levin Z, Price C, Ganor E. 1990. The contribution of sulfate and desert aerosols to the acidification of clouds and rain in Israel. Atmos Environ 24A:1143–1151.

Levin Z, Ganor E, Gladstein V. 1996. The effects of desert particles coated with sulfate on rain formation in the eastern Mediterranean. J Appl Meteor 35:1511–1523.

Levin Z, Teller A, Ganor E, Yin Y. On the interactions of mineral dust, sea salt particles and clouds—measurements and modeling study from the MEIDEX campaign. J Geophys Res, in press.

Pardess D, Levin Z, Ganor E. 1992. A new method for measuring the mass of sulfur in single aerosols particles. Atmos Environ 26A:675–680.

Posfai M, Xu H, Anderson JR, Buseck PR. 1998. Wet and dry sizes of atmospheric aerosol particles: a combined AFM-TEM study. Geophys Res Lett 25:1907–1910.

Ramirez-Aguilar KA, Lehmpuhl DW, Michel AE, Briks JW, Rowlen KL. 1999. Atomic force microscopy for the analysis of environmental particles. Ultramicroscopy 77:187–194.

Spurny NR. 1986. Physical and chemical characterization of individual airborne particles. New York: Wiley.

Vaz CMP, Herrmann PSP, Crestana S. 2002. Thickness and size distribution of clay-sized soil particles measured through atomic force microscopy. Powder Technology 126:51–58.

Wang J, Liu X, Christopher S, Reid JS, Reid E, Maring H. 2003. The effects of non-sphericity on geostationary satellite retrievals of dust aerosols. Geophys Res Lett 30:doi:10.1029/2003GL018697.